Photodiagnosis and Photodynamic Therapy 36 (2021) 102555

Contents lists available at ScienceDirect

Photodiagnosis and Photodynamic Therapy

journal homepage: www.elsevier.com/locate/pdpdt

AlPc/ZnPc-based oncological photodynamic therapy for a selective eradication of leukemic cells from ovarian tissue

Saeid Moghassemi [a], Arezoo Dadashzadeh [a], Paulo Eduardo Narcizo de Souza [b], Ricardo Bentes Azevedo [c], Christiani A. Amorim [a,*]

[a] Pôle de Recherche en Gynécologie, Institut de Recherche Expérimentale et Clinique, Université Catholique de Louvain, Brussels, Belgium
[b] Laboratory of Electron Paramagnetic Resonance, Institute of Physics, University of Brasilia, Brasilia 70910-900, Brazil
[c] Laboratory of Nanobiotechnology, Department of Genetics and Morphology, Institute of Biological Sciences, University of Brasília, Brasília DF, Brazil

ARTICLE INFO

Keywords:
Photodynamic therapy
Cancer therapy
Photosensitizer
Ovarian transplantation
Leukemia
Phthalocyanine
Photoimmunotherapy

ABSTRACT

Due to the risk of reintroducing malignant cells, autotransplantation of cryopreserved ovarian tissue is not allowed in leukemia patients. In order to restore fertility in these patients, *ex vivo* purging of ovarian fragments could be proposed as a strategy to eradicate malignant cells before grafting. Photodynamic therapy (PDT), as a clinical-approved modality, is a minimally invasive and selective therapeutic for eliminating malignant cells. The present work aims therefore to evaluate the phototoxicity of two photosensitizers (aluminum phthalocyanine (AlPc) and zinc phthalocyanine (ZnPc)) on leukemia cells. To this end, two lines of malignant cells (K562 and HL-60) and isolated ovarian stromal cells (control) were treated by PDT using a diode laser with various energy densities. Cell viability after the treatment, the amount of generated reactive oxygen species, dark toxicity of the photosensitizers, and single-cell morphology were studied. Our results demonstrated that using irradiation with the energy density of 10 J/cm^2, 1 μM AlPc could significantly reduce the viability of K562 (4.73 ± 0.14%) and HL-60 (2.74 ± 0.31%). Similarly, the viability of these cells was reduced (K562 cells: 3.84 ± 0.81%; HL-60 cells: 6.82 ± 3.21%) with 1 μM ZnPc and an energy density of 50 J/cm^2. On the other hand, these PDT protocols had no significant effect on stromal cells. These findings indicate that our approach can be a promising strategy for the safe restoration of fertility in leukemia patients. However, further studies are necessary to assess its efficiency in ovarian fragments containing malignant cells to determine their eradication rate and the effect of our treatment on the survival of stromal cells and preantral follicles.

1. Introduction

Autotransplantation of cryopreserved ovarian tissue is one of the few alternatives to restore the fertility of prepubertal girls and women who need urgent cancer care [1–3]. Unfortunately, this strategy cannot be advised for the patients diagnosed with chronic (CML) or acute myeloid leukemia (AML) due to the high risk of contamination of the ovarian tissue with malignant cells, which potentially lead to relapse of the primary disease after grafting [4–6]. One of the approaches under development for these patients is the purging of ovarian tissue from CML and AML cells before autotransplantation [7,8]. Nevertheless, this must be done selectively and without affecting follicles and ovarian stromal cells [8].

Photodynamic therapy (PDT) has received significant attention as a promising approach for cancer treatment. Compared with common strategies for cancer therapy, PDT has fewer side effects, more selectivity, and can be specifically targeted at the tumor site [9–11]. PDT uses photosensitizers (PSs), which can cause the elimination of cancer cells as soon as they are excited by laser irradiation at a specific wavelength with appropriate energy density. In the presence of oxygen, the excited PS generates singlet oxygen and other reactive oxygen species (ROS), which cause the oxidation of various biomolecules and lead to tumor cell death [12–14]. Aluminum phthalocyanine (AlPc), zinc phthalocyanine (ZnPc), and their derivatives are metal-based tetracarboxylic phthalocyanines (Table 1), known as second-generation PSs commonly used in the treatment of various cancer cell types.

This study aims to evaluate the phototoxicity efficiency of AlPc and ZnPc on the human CML K562 and AML HL-60 cell lines and isolated

* Corresponding author at: Pôle de Recherche en Gynécologie, Institut de Recherche Expérimentale et Clinique, Université Catholique de Louvain, Avenue Mounier 52, bte B1.52.02, 1200 Brussels, Belgium.
E-mail address: christiani.amorim@uclouvain.be (C.A. Amorim).

https://doi.org/10.1016/j.pdpdt.2021.102555
Received 13 July 2021; Received in revised form 30 August 2021; Accepted 24 September 2021
Available online 28 September 2021

Table 1
Structure, formula, molecular weight, and singlet oxygen quantum yield of AlPc and ZnPc, and the PS LD50 (i.e., dark toxicity) and their maximum absorbance wavelength [34–36].

AlPc	$C_{32}H_{16}AlClN_8$ 574.96 g/mol	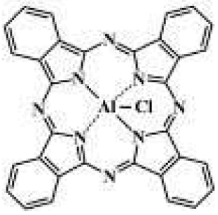	0.29	0.34	680	>10μM (EMT-6)
ZnPc	$C_{32}H_{16}N_8Zn$ 577.91 g/mol	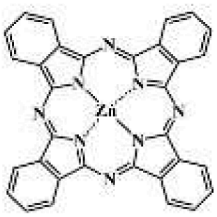	0.67	0.18	701	>5μM (MIA)

PSs: photosensitizers; AlPc: aluminum phthalocyanine; ZnPc: zinc phthalocyanine; MW: molecular weight; Φ_Δ: singlet oxygen quantum yields; Φ_F: fluorescence quantum yields; λ_{max}: wavelength of maximum absorbance; LD_{50}: light dose required for 50% cell inactivation (in vivo); **EMT-6: murine mammary carcinoma cell line; MIA: human pancreatic cancer cell line.**

human ovarian cells, as well as the effect of irradiation with different energy densities on the PDT procedure to achieve the most selective eradiation of malignant cells.

2. Materials and methods

2.1. Cell source

2.1.1. Ovarian stromal cells

The ovarian tissue biopsies were obtained after approval from the Institutional Review Board of the Université Catholique de Louvain for the use of human ovarian cortex in May 2019 (IRB reference 2012/23MAR/125, registration number B403201213872). The dissected ovary was directly transported to the laboratory in Minimum Essential Medium (MEM; 42,360–024; Gibco, Netherlands) at 4 °C. After removing the medullar part, the cortex was frozen using our routine procedure [15]. The ovarian stromal cells were isolated after thawing [15] of the ovarian tissue fragments, according to Asiabi et al. [16]. Briefly, the tissue was mechanically minced (McIlwain Tissue Chopper, Mickel Laboratory, UK), and then digested with Liberase DH (5,401,054,001; Sigma-Aldrich, Belgium) and DNAse I (10,104,159,001; Sigma-Aldrich) at 37 °C for 75 min. Then, the enzymatic digestion was halted by adding an equal amount of Dulbecco's phosphate-buffered saline (D-PBS; 14,190,144; Gibco) supplemented with 10% heat-inactivated fetal bovine serum (HI-FBS; 16,140–071; Gibco). Afterward, the suspension was filtered through 80 (NY8002500; Millipore, Belgium) and 30 μm (NY3002500; Millipore) nylon net filters and centrifuged (500 g, 10 min). The pellet was resuspended in Dulbecco's modified of Eagle's medium F-12 nutrient mixture (DMEM/F12; 21,041–025; Gibco) with 10% HI FBS and 1% of antibiotic and antimycotic (Anti-Anti; Gibco).

2.1.2. Leukemia cells

Human leukemic malignant cell lines HL-60 and K562 were purchased (98,070,106 and 89,121,407; Sigma-Aldrich) and expanded in RPMI-1640 medium (61,870–010; Gibco) supplemented with 10% HI-FBS and 1% Anti-Anti and kept in humidified condition with 5% CO_2 at 37 °C. For cell subculture, we used Accutase (A6964; Sigma). Cells at passage eight were used for this study.

Table 2
Laser parameters for irradiation using the 660 nm diode laser.

Parameter	Description/Value
Laser type	Semiconductor diode
Wavelength (nm)	660 nm
Wave emission	Continuous
Power density (mW/cm^2)	11.15 or 18.59 mW/cm^2
Energy density (J/cm^2)	10 or 50 J/cm^2
Light/plate distance (cm)	13 cm
Irradiation times	15 - 45 min

2.2. Cell culture

Ovarian stromal, K562, and HL-60 cells were in vitro cultured in a 96-well plate (Sarstedt, Germany) coated by poly-D-lysine (PDL; A3890401; Gibco). Briefly, 50 μl of 5% PDL 0.1 mg/ml in D-PBS was added to each well. After 1 h incubation at room temperature, the wells were rinsed three times by deionized water and dried for 2 h without the lid at room temperature. Then, cells were seeded (2×10^4 cells/well) and in vitro cultured for 24 h.

2.3. Photodynamic treatment

Cells were exposed to different concentrations (0, 0.005, 0.01, 0.05, 0.1, 0.5, 1 and 5 μM) of either AlPc (362,530; Sigma-Aldrich) or ZnPc (39,553; Alfa Aesar, Germany) for 2 h. Then, the medium was replaced and the cells were exposed or not to a 660 nm diode laser with the energy density of 10 or 50 J/cm^2 (Table 2) and in vitro cultured for another 24 h before analysis. All the experiments were performed in triplicate.

2.4. Cell viability assays

2.4.1. PrestoBlue assay

Treatment cytotoxicity was established by the PrestoBlue™ HS (P50200; Invitrogen, Belgium) metabolic assay, which is based on a resazurin-based solution that is cell-permeable and can be reduced inside the mitochondria of living cells to resorufin, a red fluorescent compound that can be quantitatively measured to determine cell viability. The fluorescent reaction product can be quantified using a

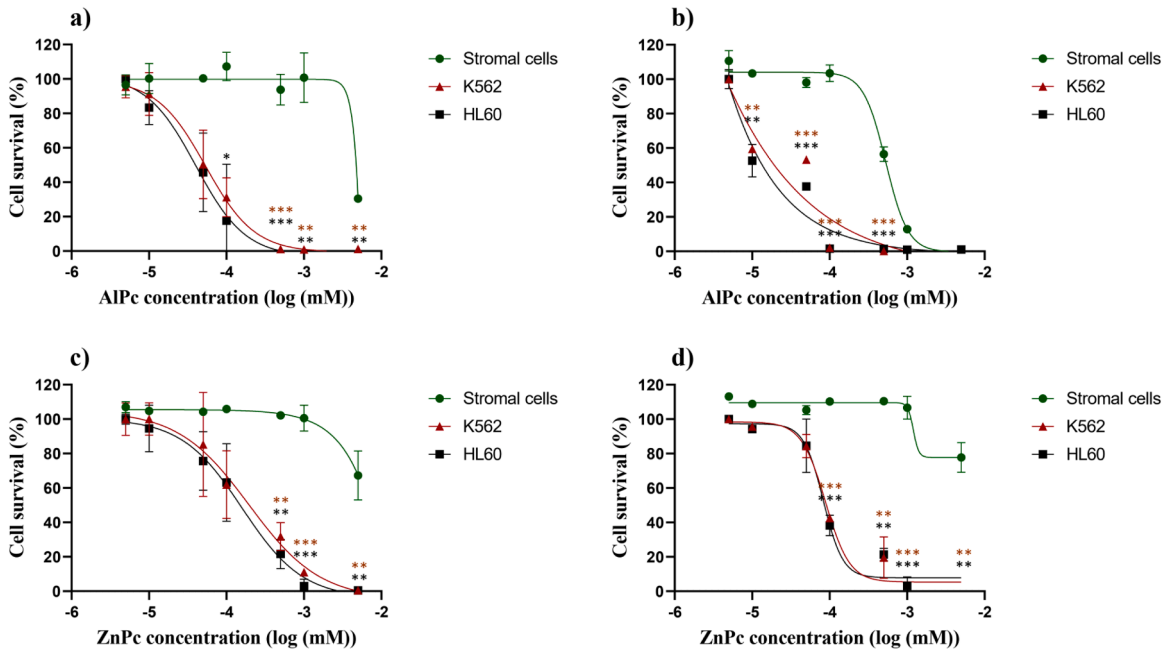

Fig. 1. Cell viability assay based on the mitochondrial activity after treatment with different concentrations (0–5 μM) of AlPc and ZnPc and irradiated energy density. AlPc-treated cells using 10 J/cm^2 (a) or 50 J/cm^2 irradiation (b) and ZnPc-treated cells using 10 J/cm^2 (c) or 50 J/cm^2 irradiation (d) (*$p < 0.05$, **$p < 0.01$ and ***$p < 0.001$).

spectrometer (Multilabel reader, Victor X4, Singapore). The medium was replaced with PrestoBlue™ reagent:cell medium (1:10 vol ratio). After 60 min incubation, cell viability was quantified by fluorescence spectroscopy at an excitation wavelength of 560 nm and emission wavelength of 620 nm. Normalization was performed using untreated cells, and wells with just medium were fixed as 100% and 0% viability, respectively.

2.4.2. LIVE/DEAD® cell staining

Cell viability was also assessed using LIVE/DEAD™ Viability/Cytotoxicity (L3224; Invitrogen) assay. For this, cells were incubated in D-PBS containing 2 mmol/l calcein-AM and 5 mmol/l ethidium homodimer-I for 45 min at 37 °C in the dark [17]. Non-fluorescent cell-permeant calcein-AM enters cells and is cleaved by esterases in live cells, producing calcein, which is well retained within live cells, generating intense and uniform green fluorescence. Ethidium homodimer-I enters cells with damaged membranes and then binds to DNA with high affinity, resulting in a 40-fold enhancement of fluorescence, producing bright red fluorescence in dead cells. After exposure to fluorescent dyes, cells were observed under an inverted fluorescence microscope (Leica DMIL, Germany). Green fluorescence was visualized in live cells (ex/em 495/515 nm) and red fluorescence in dead cells (ex/em 495/635 nm), using two different filters. The corresponding fluorescence intensities were analyzed using the ImageJ software to determine the relative fraction of live versus dead cells ($n = 3$).

2.5. Measurement of ROS generation

DCFH-DA (D399; Invitrogen) was used to calculate the efficiency of intracellular ROS production [18]. To produce sufficient ROS to indicate an efficient photocytotoxic effect, the irradiated light should exhibit appropriate spectral characteristics that were matched with the PS peak absorption wavelength [19,20]. DCFH-DA can penetrate cells and be oxidized to 2′,7′-dichlorofluorescein in the presence of ROS, which can be detected using a green fluorescence detector [21]. The DCFH-DA stock solution was made in DMSO (5 mM), processed at −20 °C, and used after a simple dilution with D-PBS. Cells were washed with D-PBS and 5 μM DCFH-DA was added. After 30 min incubation, intracellular ROS generation was analyzed using the green filter (Ex: 488 nm/Em: 525 nm) of the fluorescence inverted microscope. To measure the average intracellular fluorescence intensities, the generated ROS were quantified using ImageJ software. In an 8-bit image, there are 256 possible values from 0 to 255 for each pixel, and RGB histograms show the frequency distribution of pixel values ($n = 3$).

2.6. Cell morphology

Ovarian stromal and HL-60 cells were cultured in a PDL-coated glass-bottom 96-well plate (PBK96G-1.5–5-F; MatTek, USA) with the cell density of 1×10^4 cells/well for 24 h. After 2 h incubation with 0 or 5 μM ZnPc or AlPc, they were exposed to the diode laser with an energy density of 50 J/cm^2. Then, they were in vitro cultured for 24 h, and their morphology was visualized using super-resolution 3D microscopy (CX-A Imaging Platform; Nanolive, Switzerland) for automated 3D label-free live cell imaging.

2.7. Statistical analysis

The quantitative data were reported as mean ± SD, and the data were statistically analyzed using one-way ANOVA. P values < 0.05 were considered statistically significant. The error bars in graphs reflect a single sample standard deviation.

3. Results

3.1. The efficiency of AlPc/ZnPc to destroy leukemia cells

Based on PrestoBlue™ HS assay, AlPc appears to have more phototoxicity in comparison with ZnPc and caused a complete eradication of cancer cells for irradiated energy densities of 10 and 50 J/cm^2 using the concentrations of 0.5 and 0.1 μM, respectively (Fig. 1a,b). The AlPc-PDT process irradiated with an energy density of 10 J/cm^2 has shown no toxicity on stromal cells even at a concentration as high as 1 μM (Fig. 1a). Similarly, there was a significant difference between stromal and malignant cell viability after ZnPc-PDT treatment using both irradiation conditions (Fig. 1c, d). ZnPc demonstrated an acceptable

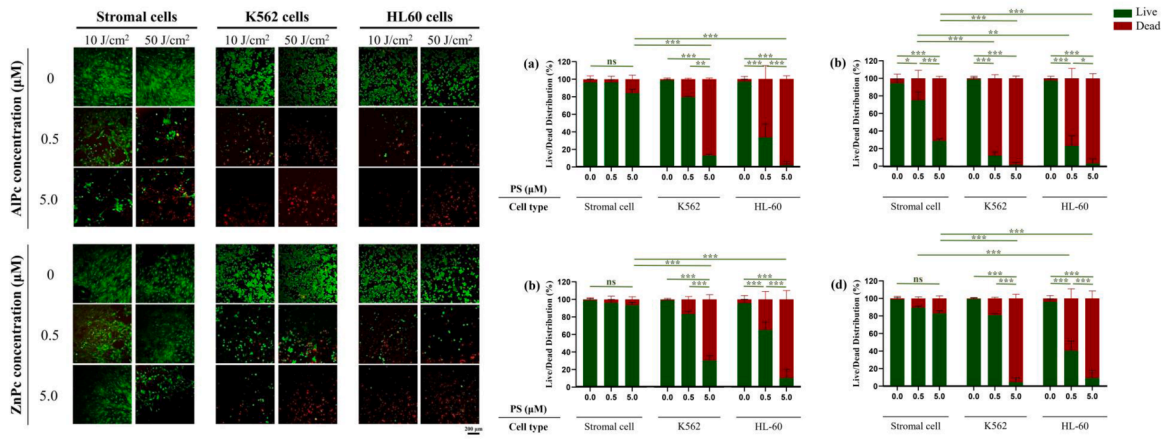

Fig. 2. LIVE/DEAD assay of human ovarian stromal, K562 and HL-60 cells after treatment with different concentrations of AlPc and ZnPc (0, 0.5, and 5 μM) and irradiated energy density and quantification of live/dead distribution. AlPc-treated cells using 10 J/cm^2 (a) or 50 J/cm^2 irradiation (b) and ZnPc-treated cells using 10 J/cm^2 (c) or 50 J/cm^2 irradiation (d) (*$p < 0.05$, **$p < 0.01$ and ***$p < 0.001$). Green cells/bars represent live cells and red cells/bars represent dead cells.

Table 3
Antiproliferative activity of AlPc/ZnPc-based PDT using exposed to the 660 nm diode laser with the energy density of 10 and 50 J/cm^2.

Cell Types	AlPc IC_{50} (μM) ± SD		ZnPc IC_{50} (μM) ± SD	
	10 J/cm^2	50 J/cm^2	10 J/cm^2	50 J/cm^2
Stromal cells	3.923 ± 0.505	0.575 ± 0.018	> 5	> 5
K562 cells	0.082 ± 0.016	0.052 ± 0.001	0.239 ± 0.101	0.145 ± 0.023
HL-60 cells	0.071 ± 0.020	0.040 ± 0.006	0.178 ± 0.066	0.137 ± 0.004

eradication of malignant cells at 1 μM. Using 1 μM ZnPc and an energy density of 50 J/cm^2 led to 96.156 ± 0.812% and 93.185 ± 3.210% inhibitory effect on K562 and HL-60 cells, respectively. However, from this dose, ZnPc starts showing phototoxicity for stromal cells when combined with irradiation with an energy density of 50 J/cm^2 (Fig. 1c, d). On the other hand, ZnPc-PDT with a concentration range of 0–1 μM has shown no significant cytotoxicity for stromal cells after both irradiation conditions (Fig. 1c,d; Fig. 2c,d).

Fig. 2 illustrates the LIVE/DEAD assay results and its quantified data, confirming PrestoBlue™ HS findings on the significant phototoxic effects in both cancer cell types using the different PS concentrations, except for K562 cells after 0.5 μM ZnPc and irradiation at 10 J/cm^2 energy density. The only considerably toxic protocol for stromal cells is 0.5 and 5 μM AlPc-50 J/cm^2 (Fig. 2b).

The antiproliferative activity of PDT using AlPc and ZnPc on stromal, K562, and HL-60 cells exposed to the 660 nm diode laser with the energy density of 10 and 50 J/cm^2 was estimated by calculating the IC_{50} (Table 3). The results show that the PS did not significantly affect the cell metabolic activity without light exposure (Fig. 3). Similarly, the quantification of LIVE/DEAD assay after PS incubation without light exposure shows no considerable difference between the treated stromal cells and their control with no treatment, demonstrating that AlPc and ZnPc have no dark toxicity on stromal cells (Fig. 4a). Furthermore, LIVE/DEAD quantification results proved that AlPc and ZnPc have no significant cytotoxicity in the absence of irradiation (Fig. 4b).

3.2. ROS generation

As shown in Fig. 5, AlPc and ZnPc resulted in strong fluorescence signals followed by irradiation at 50 J/cm^2 energy density. The fluorescence microscopy analysis of cells indicates that the ROS production after AlPc/ZnPc-based PDT with 10 and 50 J/cm^2 was significantly higher than the control (Fig. 5d). Moreover, the generation of ROS in both PSs highly depended on the exposed density of energy.

3.3. AlPc/ZnPc phototoxicity effect on cell morphology

To evaluate the impact of AlPc/ZnPc-based PDT, cell morphology was analyzed in different time points of the PDT process: (i) before and (ii) soon after PDT treatment, and (iii) 24 h after PDT treatment (Fig. 6). Ovarian stromal and HL-60 cells were treated with 5 μM AlPc or ZnPc using 660 nm diode laser exposure with the highest energy density (50 J/cm^2). According to the comparison between pre-PDT and post-PDT, AlPc/ZnPc-based PDT caused an unreturnable change in the shape of the malignant cells. Besides, the PDT procedure using 5 μM of PS

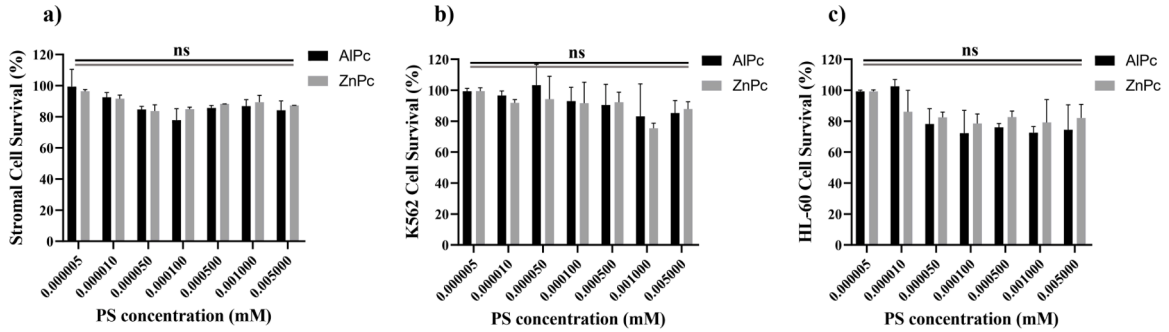

Fig. 3. Dark toxicity of AlPc and ZnPc on human ovarian stromal (a), K562 (b), and HL-60 cells (c) assessed by PrestoBlue assay (ns: not significant).

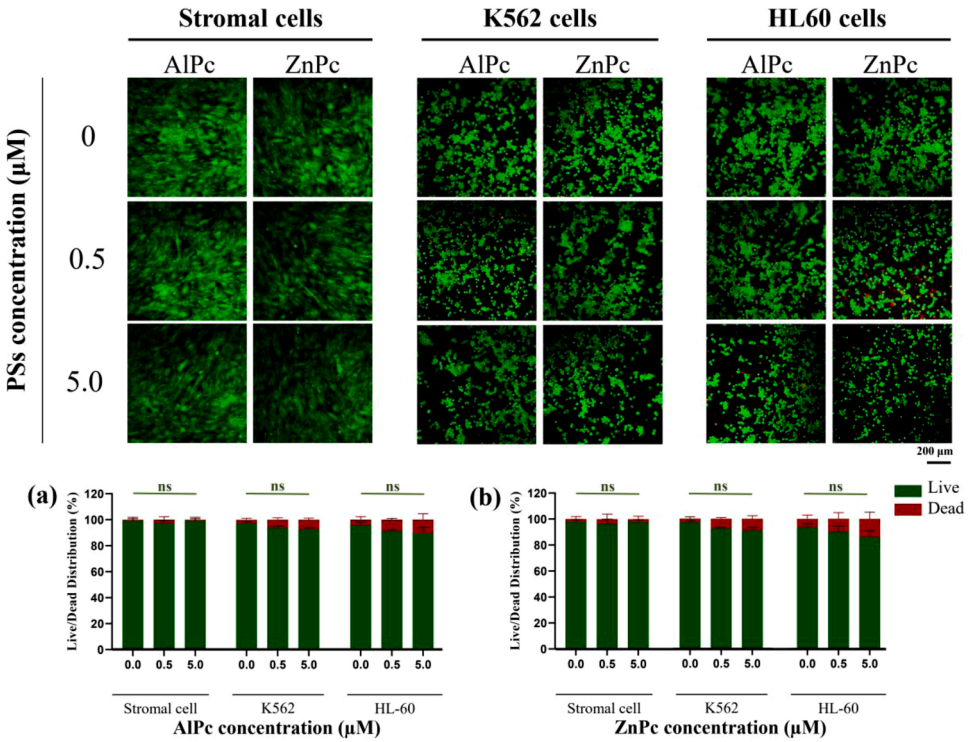

Fig. 4. Dark toxicity of AlPc and ZnPc on human ovarian stromal, K562, and HL-60 cells assessed by LIVE/DEAD assay and quantification of live/dead distribution. AlPc-treated cells (a) and ZnPc-treated cells (b) (ns: not significant). Green cells/bars represent live cells, and red cells/bars represent dead cells.

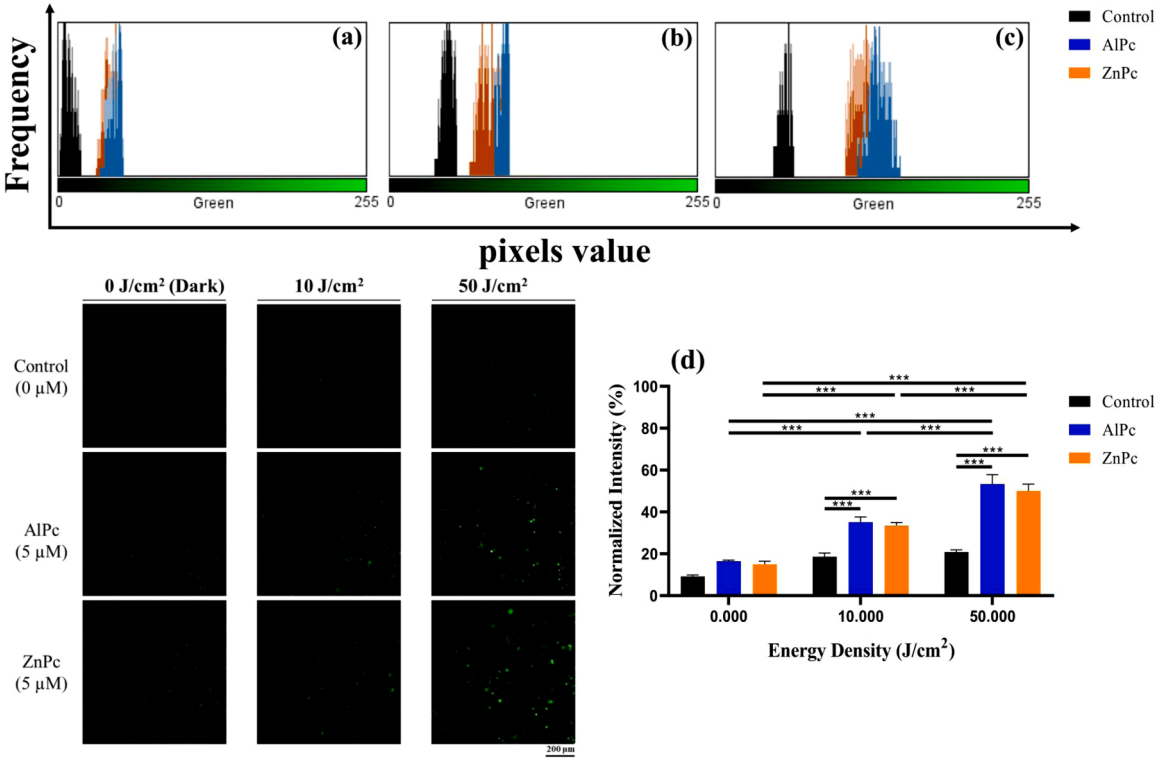

Fig. 5. Quantification of ROS generation in HL-60 cell, after PDT using 5 μM of AlPc or ZnPc exposed by different energy densities of diode laser: 0 J/cm^2 (a) 10 J/cm^2 (b) or 50 J/cm^2 (c); and normalized value of the green intensity (d). Normalization was performed using the highest and lowest pixel value as 100% and 0% intensity, respectively. (*$p < 0.05$, **$p < 0.01$ and ***$p < 0.001$).

associated with the light exposure (50 J/cm^2) causes ovarian stromal cells to become rounded up, detached, and tended to be free-floating in the culture medium (Fig. 6).

4. Discussion

PDT is a clinically approved therapeutic technique that can

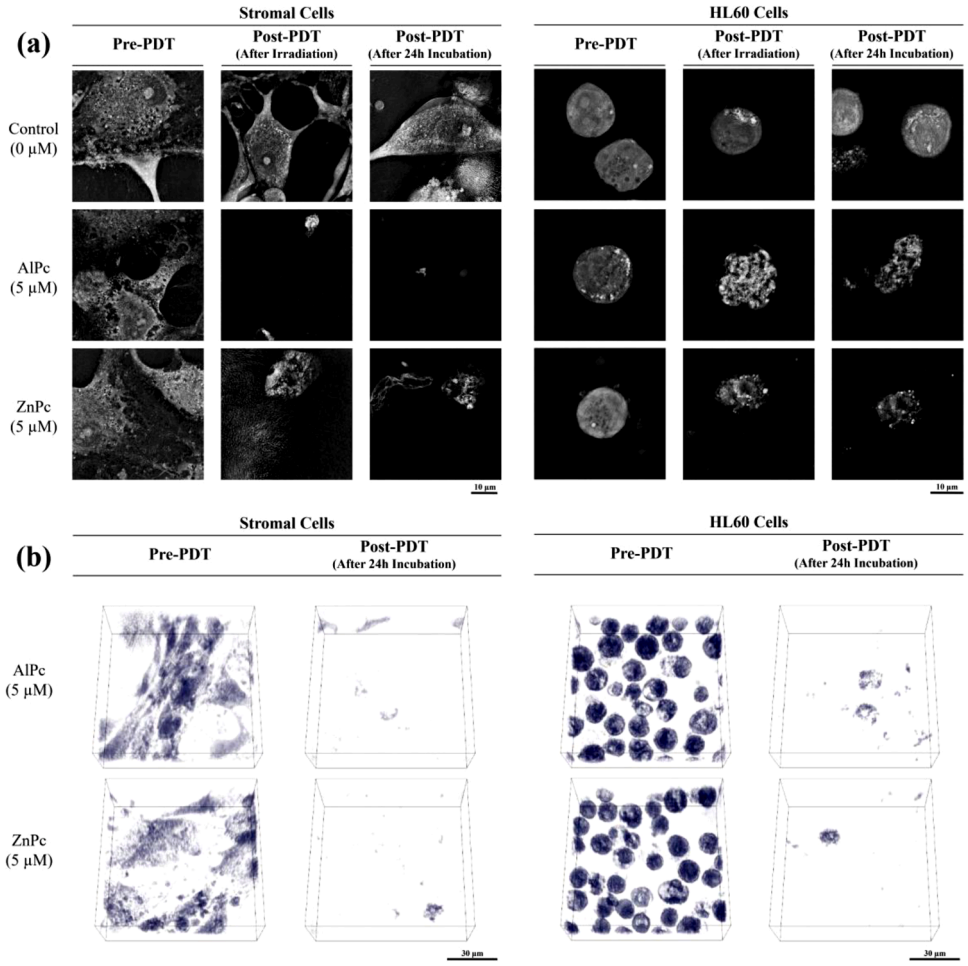

Fig. 6. HL-60 and stromal 2D (a) and 3D (b) cell morphology after PDT using 5 μM of AlPc or ZnPc exposed to the diode laser with 50 J/cm^2 in different time points of PDT process; (i) before and (ii) soon after PDT treatment, and (iii) after 24 h of PDT treatment.

selectively eliminate malignant cells while minimizing damage to healthy cells, unlike chemotherapy and genotoxic medicines, which destroy cancer cells as well as the normal tissue around them [22,23]. While we should develop a PDT approach that can successfully purge leukemic cells from ovarian tissue fragments before their auto-transplantation, it is equally necessary to ensure that the effect of this treatment should be minimal in ovarian cells. Additionally, the PDT purging process will need a selective protocol using a range of PS concentrations due to its gradient penetration in the ovarian tissue. Otherwise, the tissue borders will lose their functionality by the PS overdose and/or the cancer cells localized in the deeper areas of the tissue will not be effectively destroyed due to the lack of PS effective concentration, which could lead to the disease relapse. Therefore, in this study, we aimed to assess the efficiency of AlPc and ZnPc on the human leukemic cell lines and isolated human ovarian cells to achieve the most selective eradication of malignant cells. We observed that combining AlPc and irradiation by 10 J/cm^2 or ZnPc and irradiation by 50 J/cm^2 had no significant toxicity on ovarian stromal cells in the range of 0–1 μM. On the other hand, such treatments resulted in a considerable destructive effect on cancer cells, indicating a promising potential for the *ex vivo* PDT-purging application.

Our findings using ZnPc-PDT were in accordance with previous studies from the literature. Indeed, the IC_{50} values for ZnPc-PDT on our leukemia cell lines were similar to those reported by Doustvandi et al. [20] using a human melanoma cell line (SK-MEL-3). They also showed comparable efficacy to those observed by Feuser et al. [24], who applied ZnPc-based PDT at 47.43 ± 1.20 ng/ml on K562 cells.

Likewise, our results using AlPc-PDT on leukemia cells agreed with those on murine breast adenocarcinoma (4T1), which were exposed to similar treatment (incubation time: 105 min; light dose: 25 J/cm^2) [25]. Interestingly, we observed that while AlPc has a lower IC_{50}, it appears to be more toxic than ZnPc for all cell types. Similarly, Escobar et al. [26] reported a lower median effective dose for AlPc compared with ZnPc for the treatment of Leishmania promastigotes, using a non-ionic red laser light system (670 nm, 10 J/cm^2).

The PSs should have no toxicity in the absence of light, and a critical advantage of these phthalocyanines is that they do not exhibit substantial toxicity [27,28]. In our study, AlPc and ZnPc showed no significant cytotoxicity in the absence of irradiation for neither leukemia cell lines nor ovarian cells. In a comparable study, the metabolic activity of HeLa and HSC-3 cells was unaffected by the AlPc/ZnPc-based treatment without exposure to light [29]. This indicates that the effect of PSs was irradiation-dependent, and the remaining PS in the tissue fragments will not be toxic after transplantation.

Another benefit of AlPc and ZnPc for PDT *ex vivo* purging application is that they are active at mild wavelengths of ~674 nm, which is well within the therapeutic optical window (650–850 nm) [27]. As a result, the exposed light may be significantly absorbed by the PS while being poorly absorbed by the tissues as well as having high penetration in a biological fragment [30,31]. It is also important to bear in mind that the penetration depth of a 660 nm diode laser into human skin is 4.5–5 mm [32], which is superior to the thickness of ovarian tissue fragments (~1 mm). Therefore, while the idea of PDT *ex vivo* purging of the human ovary is highly novel, based on this information, we can presume that

such an approach can successfully be applied for *ex vivo* purging of the ovarian cortex fragments. Indeed, the tissue fragments could be easily incubated in the PS solution during transport of the ovarian biopsy to the laboratory and irradiated after preparation of the ovarian strips (~ 10 × 5 × 1 mm). While most of the fragments would be frozen, a sample could be prepared for analysis [33] to ensure that the PDT eliminated the malignant cells.

In conclusion, the present study shows Zn (II) and Al (III) phthalocyanines did not cause dark toxicity for normal cells, while 2 h incubating the cells with 5 μM AlPc/ZnPc associated with 50 J/cm^2 irradiation cause cell death and an irretrievable change in their morphology. Besides, since a selective cancer cell eradication is needed for *ex vivo* PDT-purging malignant cells from ovarian fragments, AlPc-10 J/cm^2 and ZnPc-50 J/cm^2, both in the range of 0.5–1 μM showed high potential for this regard. While such findings are promising for the safe restoration of fertility in leukemia patients, further studies are necessary to assess the efficiency of our *ex vivo* PDT purging approach in ovarian fragments containing malignant cells to determine their eradication rate as well as the effect of our treatment on the survival of stromal cells and preantral follicles.

Declaration of Competing Interest

There are no conflicts of interest to disclose.

Acknowledgments

This study was supported by grants from the Fonds National de la Recherche Scientifique de Belgique (the Excellence of Science (FNRS-EOS), number 30443682 (PhD scholarship awarded to S.M.) and FNRS-PDR Convention grant number T.0004.20 awarded to C.A.A.), and Fondation Louvain (PhD scholarship awarded to A.D.).

References

[1] J. Donnez, M.-.M. Dolmans, Fertility preservation in women, N. Engl. J. Med. 377 (17) (2017) 1657–1665.
[2] M.-.M. Dolmans, Recent advances in fertility preservation and counseling for female cancer patients, Expert Rev. Anticancer Ther. 18 (2) (2018) 115–120.
[3] E.C.R. Leonel, C.M. Lucci, C.A. Amorim, Cryopreservation of human ovarian tissue: a review, Transfusion Med. Hemotherapy 46 (3) (2019) 173–181.
[4] M.C. Chiti, M.-.M. Dolmans, L. Mortiaux, F. Zhuge, E. Ouni, P.A.K. Shahri, E. Van Ruymbeke, S.-.D. Champagne, J. Donnez, C.A. Amorim, A novel fibrin-based artificial ovary prototype resembling human ovarian tissue in terms of architecture and rigidity, J. Assist. Reprod. Genet. 35 (1) (2018) 41–48.
[5] M. McLaughlin, D. Albertini, W. Wallace, R. Anderson, E. Telfer, Metaphase II oocytes from human unilaminar follicles grown in a multi-step culture system, MHR: Basic Sci. Reprod. Med. 24 (3) (2018) 135–142.
[6] D. Meirow, Fertility preservation in cancer patients using stored ovarian tissue: clinical aspects, Curr. Opin. Endocrinol., Diabetes Obesity 15 (6) (2008) 536–547.
[7] L. Eijkenboom, C. Mulder, B. van der Reijden, N. van Mello, J. van Leersum, T. Koorenhof-Scheele, D. Braat, C. Beerendonk, R. Peek, Purging human ovarian cortex of contaminating leukaemic cells by targeting the mitotic catastrophe signalling pathway, J. Assist. Reprod. Genet. (2021) 1–18.
[8] C.L. Mulder, L.L. Eijkenboom, C.C. Beerendonk, D.D. Braat, R. Peek, Enhancing the safety of ovarian cortex autotransplantation: cancer cells are purged completely from human ovarian tissue fragments by pharmacological inhibition of YAP/TAZ oncoproteins, Hum. Reprod. 34 (3) (2019) 506–518.
[9] U. Chilakamarthi, L. Giribabu, Photodynamic therapy: past, present and future, Chem. Record 17 (8) (2017) 775–802.
[10] P. Lehmann, Side effects of topical photodynamic therapy, Hautarzt 58 (7) (2007) 597–603.
[11] S. Kwiatkowski, B. Knap, D. Przystupski, J. Saczko, E. Kędzierska, K. Knap-Czop, J. Kotlińska, O. Michel, K. Kotowski, J. Kulbacka, Photodynamic therapy–mechanisms, photosensitizers and combinations, Biomed. Pharmacother. 106 (2018) 1098–1107.
[12] S.K. Sharma, L.Y. Chiang, M.R. Hamblin, Photodynamic therapy with fullerenes in vivo: reality or a dream? Nanomedicine 6 (10) (2011) 1813–1825.
[13] M.G. Mokwena, C.A. Kruger, M.-.T. Ivan, A. Heidi, A review of nanoparticle photosensitizer drug delivery uptake systems for photodynamic treatment of lung cancer, Photodiagnosis Photodyn. Ther. 22 (2018) 147–154.
[14] T.J. Dougherty, C.J. Gomer, B.W. Henderson, G. Jori, D. Kessel, M. Korbelik, J. Moan, Q. Peng, Photodynamic therapy, J. Natl. Cancer Inst. 90 (12) (1998) 889–905.
[15] M. Gallardo, F. Paulini, A. Corral, M. Balcerzyk, C.M. Lucci, J. Ambroise, M. Merola, L. Fernandez-Maza, R. Risco, M.-.M. Dolmans, Evaluation of a new freezing protocol containing 20% dimethyl sulphoxide concentration to cryopreserve human ovarian tissue, Reprod. Biomed. Online 37 (6) (2018) 653–665.
[16] P. Asiabi, M.-.M. Dolmans, J. Ambroise, A. Camboni, C. Amorim, In vitro differentiation of theca cells from ovarian cells isolated from postmenopausal women, Hum. Reprod. 35 (12) (2020) 2793–2807.
[17] C.A. Amorim, A. Van Langendonckt, A. David, M.-.M. Dolmans, J. Donnez, Survival of human pre-antral follicles after cryopreservation of ovarian tissue, follicular isolation and in vitro culture in a calcium alginate matrix, Hum. Reprod. 24 (1) (2009) 92–99.
[18] Q. Li, W. Li, H. Di, L. Luo, C. Zhu, J. Yang, X. Yin, H. Yin, J. Gao, Y. Du, A photosensitive liposome with NIR light triggered doxorubicin release as a combined photodynamic-chemo therapy system, J. Control. Release 277 (2018) 114–125.
[19] K. Plaetzer, B. Krammer, J. Berlanda, F. Berr, T. Kiesslich, Photophysics and photochemistry of photodynamic therapy: fundamental aspects, Lasers Med. Sci. 24 (2) (2009) 259–268.
[20] M.A. Doustvandi, F. Mohammadnejad, B. Mansoori, H. Tajalli, A. Mohammadi, A. Mokhtarzadeh, E. Baghbani, V. Khaze, K. Hajiasgharzadeh, M.M. Moghaddam, Photodynamic therapy using zinc phthalocyanine with low dose of diode laser combined with doxorubicin is a synergistic combination therapy for human SK-MEL-3 melanoma cells, Photodiagnosis Photodyn. Ther. 28 (2019) 88–97.
[21] A. Grebinyk, S. Grebinyk, S. Prylutska, U. Ritter, O. Matyshevska, T. Dandekar, M. Frohme, C60 fullerene accumulation in human leukemic cells and perspectives of LED-mediated photodynamic therapy, Free Radic. Biol. Med. 124 (2018) 319–327.
[22] A. Crous, E. Chizenga, N. Hodgkinson, H. Abrahamse, Targeted photodynamic therapy: a novel approach to abolition of human cancer stem cells, Int. J. Opt. 2018 (2018).
[23] P. Agostinis, K. Berg, K.A. Cengel, T.H. Foster, A.W. Girotti, S.O. Gollnick, S. M. Hahn, M.R. Hamblin, A. Juzeniene, D. Kessel, Photodynamic therapy of cancer: an update, CA Cancer J. Clin. 61 (4) (2011) 250–281.
[24] P.E. Feuser, P.C. Gaspar, A.V. Jacques, A.C. Tedesco, M.C. dos Santos Silva, E. Ricci-Júnior, C. Sayer, P.H.H. de Araújo, Synthesis of ZnPc loaded poly (methyl methacrylate) nanoparticles via miniemulsion polymerization for photodynamic therapy in leukemic cells, Mater. Sci. Eng.: C 60 (2016) 458–466.
[25] P. Escobar, I.P. Hernández, C.M. Rueda, F. Martínez, E. Páez, Photodynamic activity of aluminium (III) and zinc (II) phthalocyanines in Leishmania promastigotes, Biomedica 26 (2006) 49–56.
[26] M.C. Rodrigues, L.G. Vieira, F.H. Horst, E.C. de Araújo, R. Ganassin, C. Merker, T. Meyer, J. Böttner, T. Venus, J.P.F. Longo, Photodynamic therapy mediated by aluminium-phthalocyanine nanoemulsion eliminates primary tumors and pulmonary metastases in a murine 4T1 breast adenocarcinoma model, J. Photochem. Photobiol. B 204 (2020), 111808.
[27] M. Broekgaarden, R. Weijer, A.C. van Wijk, R.C. Cox, M.R. Egmond, R. Hoebe, T. M. van Gulik, M. Heger, Photodynamic therapy with liposomal zinc phthalocyanine and tirapazamine increases tumor cell death via DNA damage, J. Biomed. Nanotechnol. 13 (2) (2017) 204–220.
[28] A.P. Castano, T.N. Demidova, M.R. Hamblin, Mechanisms in photodynamic therapy: part one—Photosensitizers, photochemistry and cellular localization, Photodiagnosis Photodyn. Ther. 1 (4) (2004) 279–293.
[29] J. Young, M. Yee, H. Kim, J. Cheung, T. Chino, N. Düzgüneş, K. Konopka, Phototoxicity of liposomal Zn-and Al-phthalocyanine against cervical and oral squamous cell carcinoma cells in vitro, Med. Sci. Monit. Basic Res. 22 (2016) 156.
[30] V. Monge-Fuentes, L.A. Muehlmann, R.B. de Azevedo, Perspectives on the application of nanotechnology in photodynamic therapy for the treatment of melanoma, Nano Rev. 5 (1) (2014) 24381.
[31] J. Zhang, C. Jiang, J.P.F. Longo, R.B. Azevedo, H. Zhang, L.A. Muehlmann, An updated overview on the development of new photosensitizers for anticancer photodynamic therapy, Acta Pharmaceutica Sinica B 8 (2) (2018) 137–146.
[32] E. Ruggiero, S. Alonso-de Castro, A. Habtemariam, L. Salassa, Upconverting nanoparticles for the near infrared photoactivation of transition metal complexes: new opportunities and challenges in medicinal inorganic photochemistry, Dalton Trans. 45 (33) (2016) 13012–13020.
[33] M.-.M. Dolmans, C. Marinescu, P. Saussoy, A. Van Langendonckt, C. Amorim, J. Donnez, Reimplantation of cryopreserved ovarian tissue from patients with acute lymphoblastic leukemia is potentially unsafe, Blood, J. Am. Soc. Hematol. 116 (16) (2010) 2908–2914.
[34] R. Weijer, M. Broekgaarden, M. Kos, R. van Vught, E.A.J. Rauws, E. breukink, T. M. van Gulik, G. Storm, M. Heger, Enhancing photodynamic therapy of refractory solid cancers: combining second-generation photosensitizers with multi-targeted liposomal delivery, J. Photochem. Photobiol. C 23 (2015) 103–131.
[35] L.M. Dias, F. Sharifi, M.J. de Keijzer, B. Mesquita, E. Desclos, J.A. Kochan, D.J. de Klerk, D. Ernst, L.R. de Haan, L.P. Franchi, Attritional evaluation of lipophilic and hydrophilic metallated phthalocyanines for oncological photodynamic therapy, J. Photochem. Photobiol. B 216 (2021), 112146.
[36] M. Idowu, T. Nyokong, Photophysical and photochemical properties of zinc and aluminum phthalocyanines in the presence of magnetic fluid, J. Photochem. Photobiol. A 188 (2–3) (2007) 200–206.